Hindawi Publishing Corporation
Mathematical Problems in Engineering
Volume 2007, Article ID 54212, 16 pages
doi:10.1155/2007/54212

Research Article

On Bumps and Reduction of Switching Transients in Multicontroller Systems

Joseph J. Yamé and Michel Kinnaert

Received 29 July 2006; Accepted 5 February 2007

Recommended by P. T. Kabamba

This paper is concerned with the realization and implementation of multicontroller systems, consisting of several linear controllers, subject to the bump phenomenon which occurs when switching between one controller acting in closed loop and another controller in the set of "offline" controllers waiting to take over the control loop. Based on a deep characterization of the bump phenomenon, the paper gives a novel and simple parameterization of such set of linear controllers, possibly having different state dimensions, to cope with bumps and their undesirable transients in switched-mode systems. The proposed technique is based on a non minimal state-space representation allowing a common memory and a unique dynamics shared by all controllers in that set. It also makes each initially open-loop unstable controller run in a stable way regardless of whether that controller is connected to the controlled process.

1. Introduction

Advanced control systems deal with changing operating environments and such control systems exhibit themselves as hybrid dynamical systems which mix continuous behavior with discrete and logic decisions. In these control systems, it is common that the input to the controlled process is temporarily different from the output issued by the controller, such a difference is caused by a substitution due to the instantaneous switching between different control laws. Typical instances of input substitution occur in reconfigurable control or multicontroller schemes such as those found in flight control for widening aircraft performance envelope, fault-tolerant systems, multimode systems, mode-switching from manual to automatic in industrial controllers. The discrepancy between the process input and the controller output might lead to performance degradation and instability of the closed-loop system. Solutions dealing with these problems are known as bumpless transfer techniques. The issue of bumpless transfer has been usually regarded as the same problem as that of the antiwindup problem which has attracted a tremendous research activity for several years, see, for example, [1–4] and references therein. In this paper, the bumpless transfer problem is considered for multicontroller systems, consisting of several linear controllers, with the requirement that such bumpless transfer should be multidirectional in the sense that the swapping in and out of a controller in the loop should result in a transientless input signal to the plant regardless of the switching sequence. The bump phenomenon is known to be directly related to the initial value of the output of the of-line controller to be switched on as compared to that of the active controller at the switching instant. Clearly, when these two output signals are equal or very close, "almost continuity" of the signal at the plant input is achieved, thereby allowing a "smooth" transition where undesirable transients are avoided or minimized. As in the controller windup problem [4], it has been recognized that the bump phenomenom originating from the mismatch between controllers outputs can be translated into conditions on the controllers *states* or *memories*. Indeed, controllers being dynamical systems, their state must have the correct value when a mode switching occurs, and if this is not the case, the corresponding control loops experience undesirable and harmful switching transients.

In simple mode switching where the aim is to switch from manual control to an ultimate controller in the loop, the bumpless transfer is usually unidirectional and is obtained by adding an *antiwindup* circuitry to the controller to be switched on. Graebe and Ahlén [5] pointed out the need to consider bidirectional bumpless transfer between two controllers in modern industrial control systems where it is often the case that a newly designed controller should be temporarily installed and tested during normal process operation. They derived a bumpless transition scheme by recasting the problem in an associated tracking problem where the standby controller is viewed as a dynamical system whose output should track the online control signal by means of a two-degree-of-freedom controller. Bidirectionality in their bumpless transfer scheme is obtained by adding a symmetrical second tracking loop for the other controller. A direct approach to bumpless transfer in a two-controller configuration is also considered in [6] where the problem is formulated as an optimal linear quadratic control problem yielding a feedback gain which acts as a "subcontroller" for the standby controller; unfortunately bidirectionality is not considered there. For multicontroller schemes such as found in hybrid or switched-mode systems, *multidirectional* bumpless transfer and avoidance of undesirable switching transients should be mandatory, and to achieve this the common approach consists in appending each controller with an *antiwindup* circuitry, see, for example, [7, 8]. In [7], the antiwindup circuitries are high-gains feedback loops around all idle controllers which force the controllers outputs to track the process input, whilst in [8] each controller is augmented with dynamics identical to that of the plant in order to allow the controller states to evolve in an appropriate way when the controller is not connected to the plant input. Clearly, such bumpless transfer schemes become cumbersome and hard to implement when the number of controllers is large. Note also that in the high-gain approach, the unstable zeros of the controllers limit the increase of the gains and the technique used by Zaccarian and Teel [8] might fail if a sufficiently accurate model of the plant is not available or if the plant is described by several models, each model being valid in a certain region of the operating space.

In this paper, we further characterize the bump phenomenon and identify its source in switched-mode systems. With this new insight on bumps, we derive a state-space realization for a multicontroller system in which the *memories* and the *system matrix* of the state equations are common and shared by all controllers of the switched-mode system. With such a representation, the dynamical parts of all controllers reduce to a single dynamics and by feeding back the actual process input into this single dynamics, that is, by conditioning the controllers, it is shown that we contend with the source of the bump phenomenon. As a consequence, this prevents the closed-loop dynamics to blow up or enter into unacceptable transients after modes switching. The distinctive parts of the controllers, removed from their dynamics, are realized through the static gains attached to their outputs. The parameterization technique used for the realization of the controllers is reminiscent to a classical technique for plant identification in adaptive control [9].

2. Bumpless transfer and switching transients

The noticeable manifestation of the bump phenomenon is a jump in the plant input, and most importantly a significant deterioration of the actual closed-loop performance with respect to the ideal or expected performance following a controller switching. But quite surprisingly, and to the best of our knowledge, the concept of bumpless transfer itself has never been precisely formalized [8] and it is sometimes misunderstood as noted in [10]. A common vague statement which conveys the idea of bumpless transfer is that of switching "smoothly" as possible from one controller to another where the notion of smoothness is understood in *some sense*. Different meanings can be found in the literature and one of these meanings is related to the continuity property (in the mathematical sense) of the plant input signal at the switching instants, that is, an input signal which does not experience a jump or discontinuity in time when switching between controllers [11]. Such a definition makes sense only for continuous-time systems but does not extend to discrete-time systems since it is difficult to talk about continuity in time on a discrete time setting. A slightly modified acceptation of the bumpless transfer concept is when the jump at the plant input is minimized in some way [5, 6]. However, realizing an input signal which is continuous in time or which has a small jump at the switching instants does not preclude the closed-loop system from exhibiting very poor transients with the new online controller [12]. In most switched-mode systems, switching between controls aims at realizing instantaneous or fast transitions between different modes to maintain the performance of closed-loop systems, hence jumps or abrupt changes in the input signal of the plant are actually inherent to such control strategies. However, the underlying control objective constraints should not be violated by the transients induced by such instantaneous events. Therefore, it is appropriate and meaningful to consider control switching as bumpless when the followup transients are reduced to some extent or possibly eliminated from the closed-loop system behavior albeit the occurrence of jumps in plant input signals and the performance still remains good after mode switching. This notion of bumpless transfer has been considered by Hanus [12] and was later termed "*conditioned*

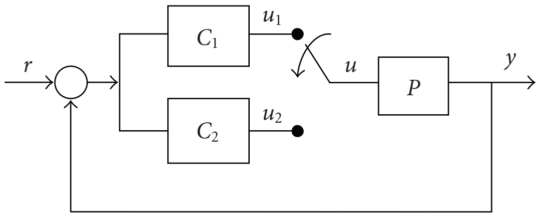

Figure 2.1. Switching from controller 1 to controller 2.

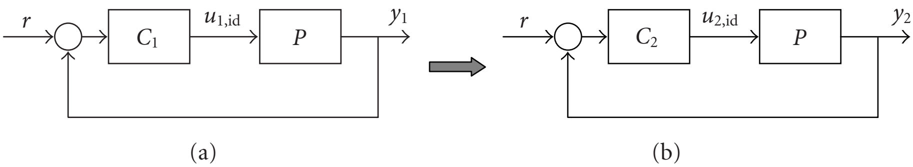

Figure 2.2. Closed-loop systems with (a) controller 1 and (b) controller 2.

transfer" by Peng et al. [10]. It is worth noticing that this notion applies indifferently to continuous-time or discrete-time systems and conveys the idea that switching should take place without perturbing the closed-loop system to depart from its desired performance. Throughout this paper, the bumpless switching problem is understood in the sense of the aforementioned idea of conditioned transfer.

Consider the switched-mode system of Figure 2.1 where we assume that the online controller in the time interval $[0,t_s)$ is controller C_1 and at time t_s, the second controller C_2 is switched in closed-loop.

The design methodologies for the controllers of such switched-mode systems are usually based on the synthesis of the closed-loop systems composed of the *individual* controllers as depicted in Figure 2.2 with the desire that the plant output signal y of the switched-mode system in Figure 2.1 be given by the ideal signal obtained by concatenating signal y_1 on $[0,t_s)$ with signal y_2 on $[t_s,\infty)$, that is,

$$y_{\mathrm{id}}(t) = \left(y_1 \overset{t_s}{\diamond} y_2\right)(t) \triangleq \begin{cases} y_1(t) & \text{for } t \in [0,t_s), \\ y_2(t) & \text{for } t \geq t_s, \end{cases} \tag{2.1}$$

where it is assumed that at time t_s, system (a) and system (b) in Figure 2.2 are in steady state. This requirement means that the closed-loop system should instantaneously reach its steady state after switching to controller C_2 so as to have a transientless signal y after controller switching. If P denotes the transfer operator of the plant, then the ouptut signal (2.1) is achieved in the switched-mode system of Figure 2.1 through the following ideal input signal to the plant:

$$u(t) = u_{\mathrm{id}}(t) = \left(u_{1,\mathrm{id}} \overset{t_s}{\diamond} u_{2,\mathrm{id}}\right)(t) \quad \text{for } t \in [0,\infty), \tag{2.2}$$

where $y_1 = Pu_{1,\mathrm{id}}$ and $y_2 = Pu_{2,\mathrm{id}}$, with $u_{1,\mathrm{id}}$, $u_{2,\mathrm{id}}$ as given in the closed-loop systems of Figure 2.2. A key feature of such ideal control u_{id} is that its segment on $[t_s, \infty)$, that is, signal $u_{2,\mathrm{id}}$ from t_s to ∞, is issued from controller C_2 which has been *constantly* connected to the plant in closed-loop. However, due to the very structure of the switched-mode system of Figure 2.1, controller C_2 can only be connected to the plant from time t_s to ∞ and consequently its history (i.e., its state trajectory) on $[0, t_s)$ has no relation with the history of the plant in that time interval. This lack of dynamical consistency between the two state trajectories up to the switching instant is the main cause of the switching transients which impair the performance of the closed-loop system when controller C_2 becomes active. Bumpless switching should aim at guaranteeing such dynamical consistency.

The actual input signal to the plant in the switched-mode system of Figure 2.1 can be written as a perturbation to the ideal input signal, that is,

$$u(t) = u_{\mathrm{id}}(t) + u_{\mathrm{tr}}(t) \quad \text{for } t \in [0, \infty), \tag{2.3}$$

where $u_{\mathrm{tr}}(t) = (0 \overset{t_s}{\diamond} (u - u_{\mathrm{id}}))(t)$ is the transient signal induced by the switching at time t_s. To see how this switching transient arises in the switched-mode system, let (F_1, G_1, H_1, J_1), (F_2, G_2, H_2, J_2), (A_P, B_P, C_P) denote the state-space realizations for controllers C_1, C_2, and plant P, respectively.

The closed-loop dynamics with controller C_2 being constantly in the loop is given by

$$\begin{pmatrix} \dot{x}_2 \\ \dot{x}_P \end{pmatrix} = \begin{pmatrix} F_2 & -G_2 C_P \\ B_P H_2 & A_P - B_P J_2 C_P \end{pmatrix} \begin{pmatrix} x_2 \\ x_P \end{pmatrix} + \begin{pmatrix} G_2 \\ B_P J_2 \end{pmatrix} r, \tag{2.4}$$

where x_2 and x_P are the state vectors of C_2 and P. The control issued by C_2 is given by the readout map

$$u_{2,\mathrm{id}} = \begin{pmatrix} H_2 & -J_2 C_P \end{pmatrix} \begin{pmatrix} x_2 \\ x_P \end{pmatrix} + J_2 r. \tag{2.5}$$

When controller C_2 is not connected to the plant in the switched-mode configuration of Figure 2.1, its output signal u_2 is still given by the right-hand side of (2.5) but the evolution of the state vectors x_2 and x_P is obtained from the dynamics

$$\begin{pmatrix} \dot{x}_2 \\ \dot{x}_P \\ \dot{x}_1 \end{pmatrix} = \begin{pmatrix} F_2 & -G_2 C_P & 0 \\ 0 & A_P - B_P J_1 C_P & B_P H_1 \\ 0 & -G_1 C_P & F_1 \end{pmatrix} \begin{pmatrix} x_2 \\ x_P \\ x_1 \end{pmatrix} + \begin{pmatrix} G_2 \\ B_P J_1 \\ G_1 \end{pmatrix} r. \tag{2.6}$$

For notation convenience, let $\xi = (x_2^T, x_P^T)^T$ denote the joint state of the controller C_2 and the plant where the superscript T stands for the transposition of the vector. The state trajectory of the closed-loop system with C_2 constantly in the loop from the time origin $t_0 = 0$ to time t and initial condition $\xi(t_0) = \xi_0$ is given by

$$\xi_{\mathrm{id}}(t) = \xi_{\mathrm{id}}(t; t_0, \xi_0, r) = \Phi(t, t_0)\xi_0 + \Theta(t, t_0) r, \tag{2.7}$$

where $\Phi(t,t_0)$ is the state transition matrix of system (2.4) and $\Theta(t,t_0)$ is an integral operator. When C_2 is not connected to the plant, the trajectory of ξ is obtained from the dynamics (2.6). This trajectory is the first block component of vector $\eta = (\xi^T, x_1^T)^T$ which is the solution of the differential equation (2.6) with initial condition $\eta_0 = (\xi_0^T, x_{1,0}^T)^T$. When the switched-mode system of Figure 2.1 transfers the control authority to controller C_2 at time t_s, the closed-loop dynamics starts evolving on $[t_s,\infty)$ according to (2.4) with initial condition $\xi(t_s^-)$ obtained from the left limit of $\eta(t)$ at t_s, that is,

$$\xi(t) = \Phi(t,t_s)\xi(t_s^-) + \Theta(t,t_s)r; \tag{2.8}$$

while for the closed-loop system with controller C_2 constantly connected to the plant, the state trajectory on $[t_s,\infty)$ is

$$\xi_{\text{id}}(t) = \Phi(t,t_s)\xi_{\text{id}}(t_s) + \Theta(t,t_s)r. \tag{2.9}$$

The switching transient is the *free motion* given by the difference between trajectories (2.9) and (2.8), that is,

$$\xi_{\text{tr}}(t) = \Phi(t,t_s)\cdot(\Delta\xi)_{t_s} \quad \text{for } t \geq t_s, \tag{2.10}$$

and the transient in the input signal to the plant is

$$u_{\text{tr}}(t) = \begin{pmatrix} H_2 & -J_2C_P \end{pmatrix}\xi_{\text{tr}}(t), \tag{2.11}$$

where $(\Delta\xi)_{t_s} = \xi_{\text{id}}(t_s) - \xi(t_s^-)$ is the mismatch between the ideal vector and actual state vector ξ at the switching instant. It is now clear that if at the switching instant t_s, the joint state $\xi(t_s^-)$ of the plant and offline controller C_2 is equal to the ideal state $\xi_{\text{id}}(t_s)$, then the input signal (2.3) to the plant in the switched-mode system will be transientless after switching even if it experiences a jump $(\Delta u)_{t_s} = u_2(t_s^+) - u_1(t_s^-) \neq 0$ at the switching instant (the arguments t_s^+ and t_s^- stand, resp., for the right and left limits at t_s of the corresponding signal).

It is interesting to note that the switching transient can be viewed as the impulse response of the dynamics $\dot{\xi} = \mathscr{A}_{\text{cl}_2}\xi$ for an impulse of "height" $(\Delta\xi)_{t_s}$ applied at time t_s and where $\mathscr{A}_{\text{cl}_2}$ is the state matrix in (2.4). The dynamical consistency between the state of the plant and the state of controller C_2 is traced in the ideal state ξ_{id} of the joint plant/controller which results from a controller constantly connected to the plant. It is also worth noticing from (2.6) that an inconsistency between these states is evidenced from the zeroed entry (2,1) of the state matrix so that the plant state evolves independently from the state of the idle controller. Since in a switched-mode system, only one controller can be effectively connected to the plant at each time, a solution to the bumpless switching problem inspired from the above analysis is to realize a virtual constant connection of all idle controllers to the plant so as to assure the dynamical consistency between the state of the plant and the states of all controllers.

3. Controllers parameterization

Assume that N single-input/single-output (SISO) linear controllers, not necessarily of the same order, have been designed for the control of a plant P as depicted in Figure 3.1

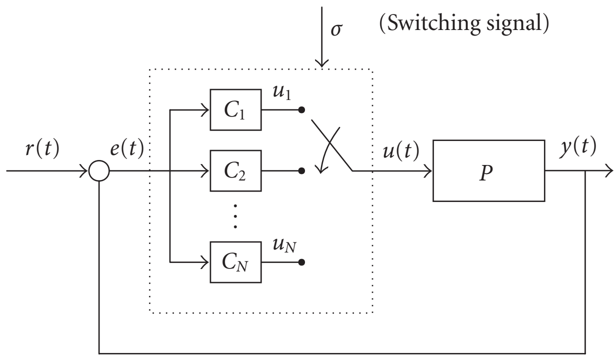

Figure 3.1. Switched-mode control system.

and that each of these controllers taken alone and connected to the plant is stabilizing. Some of these controllers might be open-loop unstable such as, for instance, controllers having an integrating action. In the feedback control system of Figure 3.1, the connection of a controller to the plant at each instant t is dependent on a switching signal $\sigma(t)$ issued by a high-level supervisory system. The switched-mode control system operates as follows: at time t, the actual input $u(t)$ to the process is given by $u(t) = u_i(t)$ if the switching signal $\sigma(t) = i$, where i takes its value in the set $\{1,2,\dots,N\}$. Assuming that a stabilizing switching policy has been designed through the synthesis of the supervisor, the main issues which remain to be solved for the switched-mode system are how to achieve bumpless transfer between the controllers in order to avoid undesirable transients and how to assure that each controller runs in a stable way even when it is not connected to the plant in closed loop.

With reference to Figure 3.1, let $e = r - y$ be the control error and denote the SISO transfer functions of the controllers by

$$C_i(s) = \frac{u_i(s)}{e(s)} = \frac{n_{C_i}(s)}{d_{C_i}(s)} \quad (i = 1,\dots,N) \tag{3.1}$$

with coprime polynomials $n_{C_i}(s)$, $d_{C_i}(s)$ and set

$$n = \max_{i=1,\dots,N} \deg\left(d_{C_i}(s)\right), \tag{3.2}$$

where $\deg(d_{C_i}(s))$ is the highest power of polynomial $d_{C_i}(s)$. Then, all transfer functions $C_i(s)$ can always be written as

$$C_i(s) = \frac{N_i(s)}{D_i(s)}, \tag{3.3}$$

where the denominators $D_i(s)$ are such that

$$\deg\left(D_i(s)\right) = n, \quad \forall i = 1,\dots,N, \tag{3.4}$$

and the numerators are of the form

$$N_i(s) = b_{i,0}s^n + b_{i,1}s^{n-1} + \cdots + b_{i,n-1}s + b_{i,n}. \tag{3.5}$$

Furthermore, each $D_i(s)$ is a monic polynomial, that is,

$$D_i(s) = s^n + a_{i,1}s^{n-1} + \cdots + a_{i,n-1}s + a_{i,n}. \tag{3.6}$$

With the transfer functions form (3.3), compared to the initial transfer functions (3.1), there might be some pole/zero cancellations introduced by the designer which should be *stable*.

Next, decompose the controllers (3.3) into a strictly proper part $C_i'(s)$ and a feedforward part $b_{i,0}$,

$$C_i(s) = C_i'(s) + b_{i,0}, \tag{3.7}$$

and write the ith controller output as

$$u_i(s) = u_i'(s) + b_{i,0}e(s) \tag{3.8}$$

with $u_i'(s)$ defined by

$$\frac{u_i'(s)}{e(s)} = C_i'(s) = \frac{N_i'(s)}{D_i'(s)} = \frac{b_{i,1}'s^{n-1} + \cdots + b_{i,n-1}'s + b_{i,n}'}{s^n + a_{i,1}'s^{n-1} + \cdots + a_{i,n-1}'s + a_{i,n}'}, \tag{3.9}$$

where $D_i'(s)$ are actually equal to $D_i(s)$. The strictly proper part $C_i'(s)$ bears all the memory (dynamics) of controller i whilst no memory information is carried out by the feedforward part $b_{i,0}$. Now using (3.9), the output signal $u_i'(s)$ can be written as

$$u_i'(s) = \frac{N_i'(s)}{\lambda(s)}e(s) + \frac{\lambda(s) - D_i'(s)}{\lambda(s)}u_i'(s), \tag{3.10}$$

where $\lambda(s)$ is an *arbitrary* monic polynomial of order n, $\lambda(s) \neq D_i'(s)$, and strictly Hurwitz, that is,

$$\lambda(s) = s^n + \lambda_1 s^{n-1} + \cdots + \lambda_{n-1}s + \lambda_n, \tag{3.11}$$

and for $p_i \in \mathbb{C}$,

$$\lambda(p_i) = 0 \Longrightarrow \operatorname{Re}(p_i) < 0. \tag{3.12}$$

Note that (3.10) results in the same input-output transfer $u_i'(s)/e(s)$ as in (3.9) but the controller is viewed as a two-input/single-output dynamical system in which one of the inputs is its output filtered by $(\lambda(s) - D_i'(s))/\lambda(s)$. The denominators of the filters in (3.10) are independent of the controllers C_i and are all equal to $\lambda(s)$. For notation convenience, let

$$\begin{aligned} \beta_i(s) &= N_i'(s) = b_{i,1}'s^{n-1} + \cdots + b_{i,n-1}'s + b_{i,n}', \\ \alpha_i(s) &= \lambda(s) - D_i'(s) = (\lambda_1 - a_{i,1}')s^{n-1} + (\lambda_2 - a_{i,2}')s^{n-2} + \cdots + (\lambda_n - a_{i,n}'), \end{aligned} \tag{3.13}$$

and introduce the constant vectors

$$\beta_i^T = \begin{pmatrix} b'_{i,n} & b'_{i,n-1} & \cdots & b'_{i,1} \end{pmatrix},$$
$$\alpha_i^T = \begin{pmatrix} \alpha_{i,n} & \alpha_{i,n-1} & \cdots & \alpha_{i,1} \end{pmatrix}, \tag{3.14}$$

with $\alpha_{i,k} = \lambda_k - a'_{i,k}$. Equation (3.10) has now the simple form

$$u'_i(s) = \beta_i^T \mathcal{F}(s) e(s) + \alpha_i^T \mathcal{F}(s) u'_i(s), \tag{3.15}$$

where the multioutput filter $\mathcal{F}(s)$ expressed in vector block form is given by

$$\mathcal{F}(s) = \frac{1}{\lambda(s)} \begin{pmatrix} 1 \\ s \\ \vdots \\ s^{n-1} \end{pmatrix}. \tag{3.16}$$

From [13, page 239], the vector (3.16) can be seen as the product

$$\mathcal{F}(s) = (sI - \mathcal{A}_\lambda)^{-1} b_\lambda, \tag{3.17}$$

where $\mathcal{A}_\lambda$ is the companion matrix whose characteristic equation is given by $\lambda(s) = 0$,

$$\mathcal{A}_\lambda = \begin{pmatrix} 0 & 1 & 0 & \cdots & 0 \\ 0 & 0 & 1 & \cdots & 0 \\ \cdot & \cdot & \cdot & \cdot & \cdot \\ \cdot & \cdot & \cdot & \cdot & \cdot \\ 0 & 0 & 0 & 0 & 1 \\ -\lambda_n & -\lambda_{n-1} & -\lambda_{n-2} & \cdots & -\lambda_1 \end{pmatrix},$$
$$b_\lambda = \begin{pmatrix} 0 & 0 & \cdots & 0 & 1 \end{pmatrix}^T. \tag{3.18}$$

A property of $\mathcal{A}$ which will be used later is that this matrix is nonsingular if and only if $\lambda_n \neq 0$ [13, page 65], which is the case here by the strict Hurwitz property (3.12) of polynomial $\lambda(s)$. From (3.15) and (3.17), the two-input/single-output dynamical systems (3.10) admit the controller canonical state-space representation

$$\begin{pmatrix} \dot{\varsigma}_1(t) \\ \dot{\varsigma}_2(t) \end{pmatrix} = \begin{pmatrix} \mathcal{A}_\lambda & 0 \\ 0 & \mathcal{A}_\lambda \end{pmatrix} \begin{pmatrix} \varsigma_1(t) \\ \varsigma_2(t) \end{pmatrix} + \begin{pmatrix} b_\lambda & 0 \\ 0 & b_\lambda \end{pmatrix} \begin{pmatrix} e(t) \\ u'_i(t) \end{pmatrix}, \tag{3.19}$$

with the outputs $u'_i(t)$ given by

$$u'_i(t) = \beta_i^T \varsigma_1(t) + \alpha_i^T \varsigma_2(t). \tag{3.20}$$

The representation (3.19)-(3.20) realizes *exactly* each of the N transfer functions $C'_i(s)$ with the main advantage that the dynamics (memories) are independent of these transfer functions and only the readout map (3.20) actually characterizes $C'_i(s)$. The dimension of the state space is $2n$, hence $2n$ memories are sufficient for describing the N dynamical systems $C_i'(s)$. Returning back to (3.8), the outputs of the controllers $C_i(s)$ are

$$u_i(t) = u_i'(t) + b_{i,0}e(t) = \beta_i^T \varsigma_1(t) + \alpha_i^T \varsigma_2(t) + b_{i,0}e(t). \tag{3.21}$$

The dynamical part of the N controllers is determined by the state matrix in (3.19). Therefore, if a transfer function C_i from e to u_i was originally unstable, the boundedness of the corresponding control signal in (3.21), whether it is connected or not to the plant, is guaranteed by the choice of $\lambda(s)$ as a strictly Hurwitz polynomial.

To proceed further, let us assume that coefficients $b_{i,0}$ are all equal to a constant b_0; the general case of nonconstant feedforward terms will follow. From the operation of the switched-mode control system, only one controller can be connected to the plant at each instant. If $\sigma(t) = m$ for some $m \in \{1,\dots,N\}$ at time t, the plant input is equal to the output of controller m and the following equations hold for controller m:

$$u(t) = u_m(t) = \beta_m^T \varsigma_1(t) + \alpha_m^T \varsigma_2(t) + b_0 e(t), \tag{3.22}$$

$$\begin{pmatrix} \dot{\varsigma}_1(t) \\ \dot{\varsigma}_2(t) \end{pmatrix} = \begin{pmatrix} \mathcal{A}_\lambda & 0 \\ 0 & \mathcal{A}_\lambda \end{pmatrix} \begin{pmatrix} \varsigma_1(t) \\ \varsigma_2(t) \end{pmatrix} + \begin{pmatrix} b_\lambda & 0 \\ -b_\lambda b_0 & b_\lambda \end{pmatrix} \begin{pmatrix} e(t) \\ u(t) \end{pmatrix}, \tag{3.23}$$

where (3.23) is obtained from (3.19) by using

$$u_m'(t) = u_m(t) - b_0 e(t) = u(t) - b_0 e(t). \tag{3.24}$$

The difference between the dynamical equations (3.23) and (3.19) is that the *actual* plant input $u(t)$ is now *fed back* in the filter, and for controller m which is effectively connected to the plant input, the above (3.22), (3.23) are completely equivalent to (3.19) and (3.21). In view of (3.23), and from the fact that all controllers outputs $u_i(t)$ ($i = 1,\dots,N$) are obtained from the $2n$ states of the same dynamics (3.19), the set of all controllers C_i can now be considered as a unique dynamical system with two inputs (e,u), $2n$ states $(\varsigma_1,\varsigma_2)$, and N outputs u_i ($i = 1,\dots,N$). In this new setting, the filter states are no longer driven by the dynamical part (u_i') of the floating outputs u_i as it should have been the case in the initial setting (see (3.19)) and these outputs u_i for all $i \neq m$ given by the readout equation (3.21) are clearly different from the outputs as computed by $u_i(s) = C_i(s)e(s)$ by the individual controllers as in Figure 2.1. However, these differences do not matter since when a switching occurs when the system is in steady state with zero tracking error and connects a new controller output, say u_l, to the plant input u, it will be shown that this new active controller output takes upon the correct values that would have resulted from $u_l(s) = C_l(s)e(s)$ or equivalently from (3.19) and (3.21) as if it has been constantly in the loop.

The multicontroller itself can now be viewed as the system, of which the input is e and the output is the input signal u to the plant as depicted in Figure 3.2, described by

$$\begin{aligned} \dot{\varsigma}(t) &= \mathcal{A}\varsigma(t) + \mathcal{B}_u u(t) + \mathcal{B}_e e(t), \\ u_i(t) &= \mathcal{C}_i \varsigma(t) + b_0 e(t) \quad \text{for } i = 1,2,\dots,N, \\ u(t) = u_{\sigma(t)}(t) &= u_i(t) \quad \text{if } \sigma(t) = i \text{ with } i \in \{1,2,\dots,N\}, \end{aligned} \tag{3.25}$$

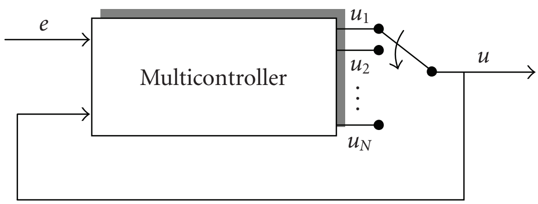

Figure 3.2. Multicontroller representation.

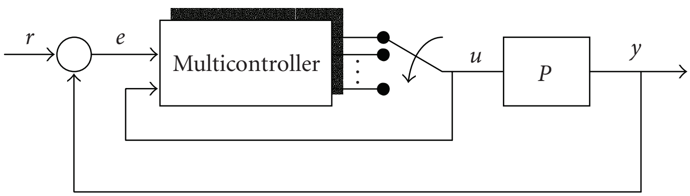

Figure 3.3. Closed-loop system with state-shared multicontroller.

where $\varsigma = (\varsigma_1^T, \varsigma_2^T)^T$ and the matrices in (3.25) are the following block matrices:

$$\mathcal{A} = \begin{pmatrix} \mathcal{A}_\lambda & 0 \\ 0 & \mathcal{A}_\lambda \end{pmatrix}, \qquad \mathcal{B}_u = \begin{pmatrix} 0 \\ b_\lambda \end{pmatrix}, \qquad \mathcal{B}_e = \begin{pmatrix} b_\lambda \\ -b_\lambda b_0 \end{pmatrix}, \qquad \mathcal{C}_i = \begin{pmatrix} \beta_i^T & \alpha_i^T \end{pmatrix}. \tag{3.26}$$

From the very nature of the filter, the state of the multicontroller is continuous at the switching instants, that is, $\varsigma(t_s) = \varsigma(t_s^-) = \varsigma(t_s^+)$ for any switching instant t_s. Moreover, the joint plant/controller state is always dynamically consistent. This is achieved through the "tracking" (via feedback) of the actual plant input which makes the state of the multicontroller correspond to the effective input/output signals (e, u). Indeed, for plant P with state vector x_P and state-space realization (A_P, B_P, C_P), the joint plant/multicontroller state of the closed-loop system of Figure 3.3 satisfies the dynamics

$$\begin{pmatrix} \dot{\varsigma} \\ \dot{x}_P \end{pmatrix} = \begin{pmatrix} \mathcal{A} + \mathcal{B}_u \mathcal{C}_\sigma & -(\mathcal{B}_u b_0 + \mathcal{B}_e) C_P \\ B_P \mathcal{C}_\sigma & A_P - B_P b_0 C_P \end{pmatrix} \begin{pmatrix} \varsigma \\ x_P \end{pmatrix} + \begin{pmatrix} \mathcal{B}_u b_0 + \mathcal{B}_e \\ B_P b_0 \end{pmatrix} r, \tag{3.27}$$

where $\mathcal{C}_\sigma = \mathcal{C}_i$ if $\sigma(t) = i$. The dynamical consistency is guaranteed by the nonzero entry $(2,1)$ of the closed-loop state matrix of (3.27) so that the evolution of the plant state is linked to the controllers state and vice versa. Since all pending controllers outputs u_i in (3.25) are computed from the same closed-loop dynamics producing state vector ς, it appears that their behavior is virtually the same as if they have been constantly connected to the plant.

Next, assume that the switching instants are such that the closed-loop system of Figure 3.3, when in any of its control modes, has already reached its steady state and the tracking error is zero ($e = 0$). Then, the equilibrium points of the joint plant/multicon-troller state in all control modes are identical. Indeed, if $P(s) = C_P(sI - A_P)^{-1}B_P$ denotes the transfer function of the plant, the input signal to the plant under the above assumption of zero tracking error in steady state is given by $u^{(0)} = P(0)^{-1}r$, where $P(0) \neq 0$ is the plant static gain which might be finite or infinite. The equilibrium state of the multicontroller system (3.25) satisfies equation

$$\mathcal{A}\varsigma^{(0)} + \mathcal{B}_u u^{(0)} = 0, \tag{3.28}$$

and from the non-singularity of matrix $\mathcal{A}_\lambda$, this equilibrium is unique and is given by

$$\varsigma^{(0)} = -\mathcal{A}^{-1}\mathcal{B}_u P(0)^{-1}r. \tag{3.29}$$

The corresponding equilibrium state of the plant is given by

$$x_P^{(0)} = -A_P^{-1}B_P P(0)^{-1}r \quad \text{if } A_P \text{ is not singular}, \tag{3.30}$$

otherwise it is the solution of the algebraic equations

$$\begin{aligned} A_P x_P^{(0)} &= 0 \\ C_P x_P^{(0)} &= r \end{aligned} \quad \text{if } A_P \text{ is singular}. \tag{3.31}$$

Thus, the equilibrium points are independent of the control modes since $\mathcal{A}$ and $\mathcal{B}_u$ are invariant with respect to the modes. In any control mode, the joint plant/multicontroller equilibrium state $\xi^{(0)} = ((\varsigma^{(0)})^T, (x_P^{(0)})^T)^T$ is the "ideal" state (see Section 2) when the steady sate has been reached in that mode. Now, referring to Section 2, it is trivial to see that when switching occurs at steady state under the zero tracking-error assumption, a transientless plant input signal is achieved from the continuity of the joint state ξ at the switching instant and from the fact that the ideal joint state $\xi_{\mathrm{id}}(t_s^+)$ to be reached after switching and the actual state $\xi(t_s^-)$ before switching are the same and are equal to $\xi^{(0)}$. Note that the input signal might experience a jump at the switching instant t_s when transferring from controller j to controller i; this jump is given by $(\Delta u)_{t_s} = u_i(t_s^+) - u_j(t_s^-) = (\mathcal{C}_i - \mathcal{C}_j)\varsigma(t_s)$, where $\varsigma(t_s) = \varsigma^{(0)}$. Therefore, a jump at the plant input does not preclude the input signal $u(t)$ to exhibit a *transientless* behavior after the switching instants. Besides, the closed-loop tracking performance is maintained after switching.

For the general case where the coefficients $b_{i,0}$ are not all identical, the following state equation for the filter is obtained using the same reasoning lines as previously developed:

$$\begin{pmatrix} \dot{\varsigma}_1(t) \\ \dot{\varsigma}_2(t) \end{pmatrix} = \begin{pmatrix} \mathcal{A}_\lambda & 0 \\ 0 & \mathcal{A}_\lambda \end{pmatrix} \begin{pmatrix} \varsigma_1(t) \\ \varsigma_2(t) \end{pmatrix} + \begin{pmatrix} b_\lambda & 0 \\ -b_\lambda b_{\sigma(t),0} & b_\lambda \end{pmatrix} \begin{pmatrix} e(t) \\ u(t) \end{pmatrix}, \tag{3.32}$$

and the N outputs $u_i(t)$ are still given by (3.21). The input matrix in the state equation (3.32) is now *dependent* on a time-varying parameter which is actually piecewise constant but undergoes a jump at the switching instants. It is worth noticing that the jump in the input matrix coefficients does not preclude the *continuity* of the state variables $(\varsigma_1, \varsigma_2)$ and it is not difficult to show that the state variables are indeed continuous functions [14].

Moreover, the joint plant/multicontroller equilibrium state $\xi^{(0)} = ((\varsigma^{(0)})^T, (x_P^{(0)})^T)^T$ is not altered since the time-varying parameter enters only into matrix $\mathcal{B}_e$ of the dynamics (3.25). This guarantees that under the same assumption as in the previous case, the multicontroller enters directly from one mode to another without any undesirable transient response.

Remarks 3.1. The derivation of the parameterization of a set of linear controllers done in the continuous-time domain in this paper extends *mutatis mutandis* to the discrete-time setting and the bumpless switching property, that is, the elimination of the switching transients, keeps its full meaning in that setting. It should be stressed that simply making the states of the control laws to be the same does not result in bumpless switching, the further step taken in transforming (3.19) into (3.23) to realize an equivalent controller is compulsory to achieve the bumpless switching property. It is this realization (3.23) which makes the pending controllers behave virtually as constantly connected to the plant. By the way, it is interesting to note that the resulting multicontroller system has an inherent implicit observer property [15] in which the shared state ς of the multicontroller includes an "observer state" for the plant. With hindsight, it is clear from this implicit observer viewpoint that the plant state and the multi-controller state will always be dynamically consistent since ς "tracks" in some way the plant state. If we regard the error signal as a generalized plant output, then the N controllers outputs u_i of (3.25) can be seen equivalently as N state-feedback control laws with feedback gains $\mathcal{C}_i$, combined with a unique "observer" producing state ς. This viewpoint corroborates the constant virtual connection of all controllers in the feedback loop.

4. Example

As a simple example illustrating the bumpless switching property of the proposed controllers parameterization, consider the first-order linear plant with transfer function $G(s) = 1/(s+1)$ controlled by a switched-mode controller with two control modes. The controllers are digitally implemented with a zero-order hold at sampling period $h = 0.01$ second. The initial controller in the loop has discrete-transfer function $C_1(z) = (z-0.95)/(z-1)$ and the control law switches at time $t = 10$ seconds to the final controller $C_2(z) = (z-0.5)/(z-1)$. The state-shared realization for these two controllers yields the following multicontroller system (in discrete time) :

$$\begin{pmatrix} \varsigma_1(k+1) \\ \varsigma_2(k+1) \end{pmatrix} = \begin{pmatrix} 0.5 & 0 \\ 0 & 0.5 \end{pmatrix} \begin{pmatrix} \varsigma_1(k) \\ \varsigma_2(k) \end{pmatrix} + \begin{pmatrix} 1 & 0 \\ -1 & 1 \end{pmatrix} \begin{pmatrix} e(k) \\ u(k) \end{pmatrix} \tag{4.1}$$

and floating control signals given by

$$\begin{pmatrix} u_1(k) \\ u_2(k) \end{pmatrix} = \begin{pmatrix} 0.05 & 0.5 \\ 0.5 & 0.5 \end{pmatrix} \begin{pmatrix} \varsigma_1(k) \\ \varsigma_2(k) \end{pmatrix} + \begin{pmatrix} 1 & 0 \\ 1 & 0 \end{pmatrix} \begin{pmatrix} e(k) \\ u(k) \end{pmatrix}. \tag{4.2}$$

The actual process input determined by the switching signal is given by $u(k) = u_{\sigma(k)}$ with $\sigma(k) \in \{1,2\}$. Figures 4.1 and 4.2 show the process output, process input (actual control), and pending controllers output signals for the two different implementations of the switched-mode controller. Note that in the direct implementation (structure of

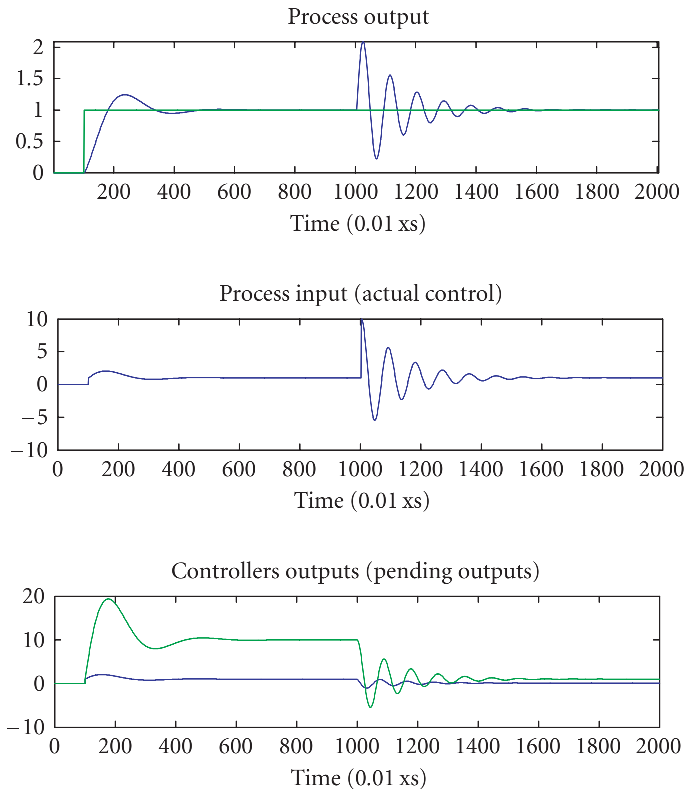

Figure 4.1. Simulation results for the direct implementation of the multicontroller.

Figure 3.1), the control system experiences an undesirable transient which significantly deteriorates the tracking performance after switching. The state-shared multicontroller (structure of Figure 3.3) shows successful bumpless switching without any transients after switching and it is worth noticing how the pending controller output tracks the actual process input.

5. Conclusion

In this paper, a characterization of the bump phenomenon in switched-mode systems has been derived in terms of the mismatch between the joint plant/controller states before and after mode switching. Based on this characterization, a state-space realization achieving bumpless switching for a given multicontroller system has been proposed using a common memory obtained through a simple parameterization of all controllers. Besides the bumpless transfer property of the realization, the dimension of the common memory, that is, the number of states shared by the controllers, is independent of the cardinality of the set of controllers. This fact is important when the number of controllers is large such as in reconfigurable control for fault-tolerant systems or in multiple operating regime

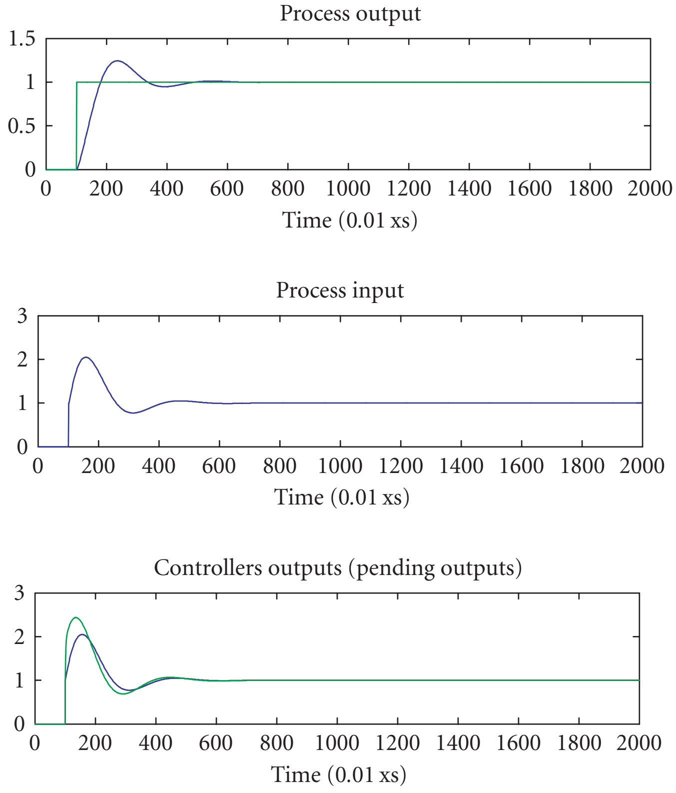

Figure 4.2. Simulation results for the state-shared multicontroller.

systems. Moreover, the common dynamics of the controllers, apart from being stable, can be choosen arbitrarily and independent of the controlled plant. Note that in most bumpless switching schemes, the controllers dynamics are augmented with observers or models of the controlled plant which make these schemes hardly applicable to plant with multiple models. The proposed bumpless switching solution which is independent of the process model is therefore particularly indicated in controller reconfiguration following dynamic changes in the controlled process. In addition to providing a parameterization of all controllers, the canonical form of the controllers state equations also simplifies the real-time implementation of the multicontroller.

Acknowledgment

This work was supported in part by the European Project IFATIS "Intelligent Fault Tolerant Control in Integrated Systems" under the Information Society Technology Research Program EU-IST-2001-32122 during the stay of the first author at the Universté Libre de Bruxelles, Belgium.

References

[1] K. J. Aström and B. Wittenmark, *Computer-Controlled Systems: Theory and Design*, Prentice-Hall, Englewood Cliffs, NJ, USA, 1984.

[2] Y. Eun, C. Gökçek, P. T. Kabamba, and S. M. Meerkov, "An LQG approach to systems with saturating actuators and anti-windup implementation," *Mathematical Problems in Engineering*, vol. 8, no. 4-5, pp. 311–321, 2002.

[3] A. H. Glattfelder, Y. Ohta, E. Mosca, and S. Weiland, Eds., "Special issue on "Anti-windup control"," *European Journal of Control*, vol. 6, no. 5, 2000.

[4] R. Hanus, M. Kinnaert, and J.-L. Henrotte, "Conditioning technique, a general anti-windup and bumpless transfer method," *Automatica*, vol. 23, no. 6, pp. 729–739, 1987.

[5] S. F. Graebe and A. L. B. Ahlén, "Dynamic transfer among alternative controllers and its relation to antiwindup controller design," *IEEE Transactions on Control Systems Technology*, vol. 4, no. 1, pp. 92–99, 1996.

[6] M. C. Turner and D. J. Walker, "Linear quadratic bumpless transfer," *Automatica*, vol. 36, no. 8, pp. 1089–1101, 2000.

[7] M. Green and D. J. N. Limebeer, *Linear Robust Control*, Prentice-Hall, Englewood Cliffs, NJ, USA, 1995.

[8] L. Zaccarian and A. R. Teel, "A common framework for anti-windup, bumpless transfer and reliable designs," *Automatica*, vol. 38, no. 10, pp. 1735–1744, 2002.

[9] S. Sastry and M. Bodson, *Adaptive Control: Stability, Convergence, and Robustness*, Prentice-Hall, Englewood Cliffs, NJ, USA, 1989.

[10] Y. Peng, D. Vrancic, and R. Hanus, "Anti-windup, bumpless, and conditioned transfer techniques for PID controllers," *IEEE Control Systems Magazine*, vol. 16, no. 4, pp. 48–57, 1996.

[11] A. B. Arehart and W. A. Wolovich, "Bumpless switching controllers," in *Proceedings of the 35th IEEE Conference on Decision and Control*, vol. 2, pp. 1654–1655, Kobe, Japan, December 1996.

[12] R. Hanus, "Systèmes d'Anti-Emballement des Régulateurs," in *Systèmes de Régulation*, A. Rachid, Ed., pp. 55–83, Masson & Cie, Paris, France, 1996.

[13] C.-T. Chen, *Linear System Theory and Design*, Saunders College, New York, NY, USA, 1984.

[14] R. Bellman and K. L. Cooke, *Modern Elementary Differential Equations*, Dover, New York, NY, USA, 2nd edition, 1995.

[15] K. S. Walgama and J. Sternby, "Inherent observer property in a class of anti-windup compensators," *International Journal of Control*, vol. 52, no. 3, pp. 705–724, 1990.

Joseph J. Yamé: Centre de Recherche en Automatique de Nancy (CRAN), (UMR 7039),
Faculté des Sciences et Techniques, Nancy-Université, BP 239, Boulevard des Aiguillettes,
54506 Vandoeuvre Cedex, France
Email address: joseph.yame@cran.uhp-nancy.fr

Michel Kinnaert: Service d'Automatique et d'Analyse des Systèmes, Université Libre de Bruxelles,
CP 165/55, Avenue F. D. Roosevelt 50, 1050 Brussels, Belgium
Email address: michel.kinnaert@ulb.ac.be

Special Issue on Time-Dependent Billiards

Call for Papers

This subject has been extensively studied in the past years for one-, two-, and three-dimensional space. Additionally, such dynamical systems can exhibit a very important and still unexplained phenomenon, called as the Fermi acceleration phenomenon. Basically, the phenomenon of Fermi acceleration (FA) is a process in which a classical particle can acquire unbounded energy from collisions with a heavy moving wall. This phenomenon was originally proposed by Enrico Fermi in 1949 as a possible explanation of the origin of the large energies of the cosmic particles. His original model was then modified and considered under different approaches and using many versions. Moreover, applications of FA have been of a large broad interest in many different fields of science including plasma physics, astrophysics, atomic physics, optics, and time-dependent billiard problems and they are useful for controlling chaos in Engineering and dynamical systems exhibiting chaos (both conservative and dissipative chaos).

We intend to publish in this special issue papers reporting research on time-dependent billiards. The topic includes both conservative and dissipative dynamics. Papers discussing dynamical properties, statistical and mathematical results, stability investigation of the phase space structure, the phenomenon of Fermi acceleration, conditions for having suppression of Fermi acceleration, and computational and numerical methods for exploring these structures and applications are welcome.

To be acceptable for publication in the special issue of Mathematical Problems in Engineering, papers must make significant, original, and correct contributions to one or more of the topics above mentioned. Mathematical papers regarding the topics above are also welcome.

Authors should follow the Mathematical Problems in Engineering manuscript format described at http://www.hindawi.com/journals/mpe/. Prospective authors should submit an electronic copy of their complete manuscript through the journal Manuscript Tracking System at http://mts.hindawi.com/ according to the following timetable:

Manuscript Due	March 1, 2009
First Round of Reviews	June 1, 2009
Publication Date	September 1, 2009

Guest Editors

Edson Denis Leonel, Department of Statistics, Applied Mathematics and Computing, Institute of Geosciences and Exact Sciences, State University of São Paulo at Rio Claro, Avenida 24A, 1515 Bela Vista, 13506-700 Rio Claro, SP, Brazil; edleonel@rc.unesp.br

Alexander Loskutov, Physics Faculty, Moscow State University, Vorob'evy Gory, Moscow 119992, Russia; loskutov@chaos.phys.msu.ru